SciMedCentral

Chemical Engineering & Process Techniques

Review Article

Theoretical Investigation of OPV5's Transport Properties in the Coulomb Blockade Regime

Idunn Prestholm, Stine T. Olsen, Thorsten Hansen, and Kurt V. Mikkelsen

Department of Chemistry, University of Copenhagen, Denmark

***Corresponding author**

Kurt V. Mikkelsen, Department of Chemistry, University of Copenhagen, Universitetsparken 5, 2100 København Ø, Denmark. Email: kmi@chem.ku.dk

Submitted: 04 April 2022

Accepted: 31 April 2022

Published: 31 April 2022

ISSN: 2333-6633

Keywords

- Theoretical Investigation
- Coulomb blockade
- Electrochemistry

Abstract

Recent knowledge of the details of molecular transistors provides the basis for investigating the electrochemistry of single molecules. Exploration of the harlequin patterns of the Coulomb blockade diamonds of molecules is a path for obtaining knowledge of the redox chemistry of single molecules. A combined QM/MM method is used to calculate the properties of a paraphenylenevinylene oligomer, OPV5, in a gold junction. Subsequent construction of the Coulomb blockade diamonds is performed based on a simplified theoretical description of the experimental set-up. The theoretical investigations provide knowledge about the actual molecular structure and orientation between the two electrodes. Moreover, the study reflects the strength of the fast, and simple, QM/MM approach, by producing results that are comparable to what is measured experimentally. The single molecule redox chemistry of the OPV5 molecule is discussed based on the calculations, and compared to experiment. The study show evident resemblance to experiment. Furthermore, it reveals chemical changes of OPV5 when OPV5 is exposed to high voltages.

INTRODUCTION

Recent developments in the field of molecular electronics has enabled us to investigate single molecule break junctions with one molecule bridging two electrodes. Experimental methods such as STM, break junctions and other single-electron transistor devices [1], enable us to explore in detail the transport of electrons though molecules at the single molecule level. The idea of a sin- gle molecule device was first proposed in 1974 by Aviram and Ratner [2], in the form of a single molecule rectifier. Today, we envision applications including transistors, molecular high-density memories, switches, and solar cells [3-6]. Molecules having inter- esting internal properties or dynamics, such as switching, optical response, or mechanistic changes [7-12], are advantageous for use in single molecule electronics. The fact that the properties of these molecules can be tuned to have specific characteristics and this will form the basic building blocks for designing future electronics [9,13-20].

If a molecule is weakly coupled to the electrodes, the discrete energy levels of the molecule will maintain, and the charged states will have relatively long lifetimes, hence, the electron can be localized. This will result in charged states of a molecule, which are induced by external potentials. This is often refereed to as the Coulomb blockade regime, and experimentally this is observed as a harlequin pattern in the conductance, i.e. the conductance is suppressed inside the diamonds. The diamonds are known as Coulomb blockade diamonds.

Experiments performed by Kubatkin et al. [1], concerned junction measurements for a single OPV5 molecule sandwiched in between two gold electrodes (Figure 1). Geometrical factors of the setup are considered in the calculations, which are discussed with respect to chemical features of the system, in addition we make comparisons with the experimental results. This study supports and verifies the findings of Kubatkin et al., in addition to revealing surprising chemical features of OPV5 at high voltages.

THEORETICAL APPROACH TO THE MOLECULAR TRANSPORT JUNCTION

The molecular transport junction is described as a molecule bridged between two electrodes, namely the source and the drain. The third gate electrode is coupled capacitively to the system, and will affect the energy levels of the molecule. The energy levels of the molecule are resembled by their redox states. Thus, the gate voltage does not have to be included in the calculations, as it is included in the calculation of the different redox states of the molecule.

We assume that the applied bias is symmetric, hence, the chemical potential of the left and right electrode are shifted equally, however, with opposite signs. Hence,

$$\mu L / R = -W \pm 1/2eVsd \quad (1)$$

where V_{sd} is the applied bias voltage.

At zero bias, electrons enter the molecule with the energy -W relative to vacuum. W is the work function of the electrode, and is dependent on both geometry of the surface, and the Fermi

Figure 1 A schematic drawing of the OPV5-P molecule in junction. The van der Waals radii of gold are included.

energy of the metal. The work function is accessible via photon photoe- mission spectrospcopy, however, for these calculations a literature value for the [11], surface of gold is used [21]. For an electron to be able the leave the electrode and move to the molecule, the work function has to match the ionization potential of the molecule. Thus,

$$-W = -\Delta_q E = E_q + 1 - E_q \tag{2}$$

Here, E_q is defined as the sum of the energy of the molecule with charge q, and the polarization energy. ΔqE is always greater than zero.

The total Hamiltonian of a molecular transport junction can be written as,

$$H = H_{mol} + H_{gold} + V_{\text{int}} \tag{3}$$

where V_{int} is the coupling between the gold particles and the molecule, including electrostatic and polarization interactions.

However, the treatment is restricted to the weakly coupled regime; thus, the molecule is not covalently coupled to the electrodes. Hence, the charging of the molecule occurs as a tunneling event and we have a single electron transfer taking place from one electrode to the molecule presented as an external potential, acting on the molecule. Now, the effective molecular Hamiltonian can be written as the original molecular Hamiltonian plus a term which describes the change in the electron density of the molecule, in the presence of the leads, Consequently, the leads are rep- resented as an external potential, acting on the molecule. Now, the effective molecular Hamiltonian can be written as the original molecular Hamiltonian plus a term which describes the change in the electron density of the molecule, in the presence of the leads

$$H_{mol}^{eff} = H_{mol} + \int dr \rho_{mol}(r)\phi^{ext}(r). \tag{4}$$

The external potential can be separated into two terms

$$\phi^{ext}(r) = \phi^{pol}(r) + \phi^{bias}(r). \tag{5}$$

The term $\varphi^{pol}(\mathbf{r})$, includes polarization effects from the leads, screening the molecular charge, and the term $\varphi^{bias}(\mathbf{r})$ describes the electric field from an arbitrary and general applied bias voltage. We will later approximate it using a simplified expression for the utilizied bias V_{sd} in the calculations. The total external poten- tial and the bias potential fulfills the Poisson equation. This can be utilized in the calculation of the redox energies and polariz- abilities. When a bias is applied, a shift in the energy of the redox state occurs. This shift is described by the equation,

$$E_q(\phi^{bias}(r)) - E_q^{vac} = \int dr \rho^{mol}(r, \phi^{bias})\phi^{bias}(r) \tag{6}$$

An expansion of $\varphi^{bias}(\mathbf{r})$ around the point $\mathbf{r0}$ will give

$$\begin{aligned} &\int dr \rho^{mol}(r, \phi^{bias})\phi^{bias}(r) \\ &= \int dr \rho^{mol}(r, \phi^{bias})\phi^{bias}(r_0) \\ &+ \int dr \rho^{mol}(r, \phi^{bias})(r - r_0)\nabla\phi^{bias}(r_0) \\ &= q\phi^{bias}(r_0) - \mu(r_0)F(r_0), \end{aligned} \tag{7}$$

where q is the charge, and the vector μ(r0) is the molecular dipole vector. The second term is a scalar product, −μ(r0)F(r0), between the vector of the molecular dipole and the electric field vector. The term is similar to the expression for the energy of a dipole in an electric field, F(r0).

The applied voltage is assumed to be divided equally between the two electrode. The surfaces of the electrodes are parallel, and treated as plate capacitors, thus, the molecule is exposed to a homogeneous electric field on the form, F = Vsd /d. The molecular levels are dependent on the field. This field-dependency is written as a field-dependent molecular dipole, which is expanded to first order. We assume that the presence of a nearby gate electrode changes the environment of the molecule and we adopt the approximation that molecule feels a constant potential that shifts linearly with the gate bias, Vg, and thereby we that Eq(Vg) = Eq + qKVg. The constant K is connected to the geomet- rical details of the experiment and presently it is not immediately accessible by experiment. Taking the two biases into account, one could write the equations describing the lines of the Coulomb diamonds. The equation

$$V_{sd} = \frac{d^2}{\Delta\alpha}\left[\pm\frac{1}{2} \pm \sqrt{\frac{1}{2}e^2 + \frac{2\Delta\alpha}{d^2}(\Delta E - W + eKV_g)}\right], \tag{8}$$

describes the crossing of the lines outlining two adjacent Coulomb diamonds [22]. The inter-electrode distance is denoted d, $\Delta\alpha/\Delta E$ is the difference in polarizability/energy of states with charge q and q+1, e is the electron charge, and K is a geometrical factor from the experimental set-up [22-24]. Taking the limit of the polarizability going to zero, we find the height of the diamond equals ^{2} times the addition energy which is given as

$$E^{add,junc} = E_{q-1} + E_{q+1} - 2E_q \tag{9}$$

This equation can also be used to describe the diamonds when

$\Delta\alpha$ is excluded. We also note that the addition energy is given by the ionization potential minus the electron affinity **?** which makes sense since electrons are removed and added to the molecular system. Having established these equations, the harlequin pattern can be constructed from the calculated QM/MM redox energies. The diamonds will occur in order q=+3 to q=-3 from left to right in the Harlequin pattern.

COMPUTATIONAL METHOD

We have in these studies considered the chemical features

of OPV5 sandwiched between two gold clusters (Figure 1), with emphasis on construction and analysis of the Coulomb blockade dia monds in the weak coupling regime. Different surface to molecule distances, and rotations of the molecule in the junction are inves- tigated. Experiments cannot supply precise distances and molecular rotations, thus, different geometric situations are considered to be able to compare calculations to experimental observations. However, with respect to rotation in the junction, one expect the molecule to be placed orthogonal to the electrodes, on average. Calculations are performed on the bare OPV5 and OPV5 with protecting groups, which are referred to as OPV5-N ((E,E)- 1,4- bis{4-{(E)-4-thiostyryl}}benzene) and OPV5-P ((E,E)-1,4-bis{4-{(E)-4-(tert-butylthio)styryl}}benzene), respectively. A study by Danilov et al. [25], on the very similar OPV3 compound without protecting groups showed that thiol end-groups actually couple to the electrode, thus inhibit the charges to be localized on the molecule, and therefore no Coulomb diamonds are observed. The tert-butyl protecting groups create an energy barrier, and thereby ensure weak molecule-electrode coupling. The tunneling barriers that occur due to this weak coupling are the dominating factor for the observation of the Coulomb blockade diamonds.

The energies, Eq, of a range of redox states of OPV5 are calcu- lated using a combined QM/MM approach. The essential equations of the method are presented in Section 2. The molecular geometry and properties are first calculated using quantum mechanics (DFT). Subsequently, the molecules are perturbed by the electrodes, which are represented as two clusters of MM atoms that are assigned with atomic polarizabilities. The damping mechanism between the MM induced dipole moments and the QM electric field at the polarizable MM sites is utilized in the calculations in order to avoid Coulombic explosions where the induced dipole moments get unphyisically large [26]. The calculations are performed in a self-consistent manner, such that the screening of the molecular charge distribution by the polarization of the electrode is included in the calculated energies.

Calculations are performed using the quantum chemistry program Dalton [27], using the long-range corrected exchange-correlation functional CAM-B3LYP [28], and the correlation consis- tent basis-set cc-pVDZ [29]. It was not possible to obtain results using larger basis sets due to computational resources and con- vergence problems. The molecular geometries are the ones from a geometry optimization in vacuum and the charged states are the energetically lowest ones for the given redox state. The molecule is placed perpendicular to the [111] gold hemispheres, that is taken from a bulk FCC crystal. The hemispheres contain 526 gold atoms and each gold atom is assigned a polarizability of 31.04a.u. [30].

Calculations are performed for 9 redox states with charges ranging from +4*e* to -4*e*, which represent a simple alternative to a more elaborate charge localization such as constrained DFT. The Coulomb blockade diamonds are constructed based on equations presented in Section 2. For a more detailed description of the computational work our previous work can be consulted [22-24]. Some of the calculations did not converge and therefore we ob- tained the relevant results for these calculations from linear least squares fittings to the remaining data.

Calculations are performed at three different molecule to elec- trode distances: 3.6Å, 3.8Å, 4.0Å, and 4.2Å and three rotations: 30 ˚ , 60 ˚ , and 90 ˚ . This is to ensure the best possible resemblance to the experimental measurements, where one commonly average over several measurements.

RESULTS

The system of interest is depicted in Figure 1. Calculations on OPV5 were performed both with and without protecting tert-butyl groups. Tert-butyl groups are suggested by Kubatkin et al. [1], to work as protecting groups to prevent covalent binding from the thiol end groups to the gold electrodes. However, the effects of the high gate and bias voltage on the protecting groups is not known. To ensure the best resemblance to experiment the calcu- lations are performed at 4 linker distances and 4 rotations of the molecule in the junction.

Calculations are performed using the CAM-B3LYP functional [28], and the double zeta correlation consistent basis set cc-pVDZ [29]. The choice of functional and basis-set is based on a small bench- mark study, and previous work using this QM/MM method.

The calculated addition energies of the redox states are listed in Table 1. Addition energies are calculated according to Eq.(9). We observe that calculated addition energies of OPV5-P ((E,E)-1,4-bis4-(E)-4-(tert-butylthio)styrylbenzene) and OPV5-N ((E,E)- 1,4-bis4-(E)-4-thiostyrylbenzene) in vacuum, and in junction do not follow an obvious pattern. It is clear that the gold nanoparticles have an influenze on the addition energies for all the distances but it is also clear that the gold nanoparticles have very little effect on the addition energies when the molecules have been rotated 90 degrees. Especially, we note that the differences between the vacuum and junction do not follow an obvious pattern. The quantitative numbers from the calculations are not in perfect agreement with the experimental data. However, we have previously shown that calculations using this QM/MM model resemble trends in the Coulomb blockade diamonds very well [22,31]. The harlequin patterns of Coulomb blockade diamonds, depicted in Figure 2, are constructed using Eq. (8). Thereby the calculated redox energies are represented in a format that connects directly to the experiment, where the addition energy corresponds to half the height of the diamond. One interesting feature, is that the states are not evenly distributed along the Vg axis, which indicates that the charging event is not dominated by Coulomb charging effects alone. When the molecule is affected by the polarizability of the gold clusters, the addition or removal of an electron is not simply determined by a change in the electrostatic energy, which is the case for simple quantum dots. The charging event also involves occupation of quantum mechanical states, which for molecules are descrete energy levels, contrary to the simple metal island seen in quantum dots, where the density of states is continuous [32].

The Coulomb blockade diamonds of OPV5-P (Figure 2), remain unchanged when changing the gold to linker distance, and the rotation of the molecule in the junction. However, rotating or changing the gold to linker distance of OPV5-N in the junction, changes the diamonds drastically. As seen in Table 1, shrinkage percent goes from 60% from calculations at 3.6Å to 3.1% for calculations with the molecule placed parallel to the junction.

Table 1: Calculated addition energies of OPV5-P ((E,E)- 1,4-bis{4-{(E)-4-(tert-butylthio)styryl}}benzene) and OPV5-N ((E,E)-.

		OPV-5N			OPV-5P	
3.6 Å	*Eadd,vac*	*Eadd, junc*	Diff. (%)	*Eadd,vac*	*Eadd, junc*	Diff. (%)
-3	3.909	3.317	15.2	1.488	1.353	9.1
-2	2.375†	2.474†	-4.2†	1.772	1.589	10.3
-1	2.702*	2.339*	13.5 *	1.948	1.841	5.5
0	0.794†	0.317†	60.0 †	5.355	5.269	1.6
1	2.401	2.099	12.6	1.737	1.571	9.6
2	1.853	1.616	12.8	1.202	1.012	15.8
3	3.586	3.451	3.8	1.911	1.806	5.5
3.8 Å						
-3	3.969	3.478	12.4	1.486	1.348	9.3
-2	2.337†	2.394†	-2.4†	1.762	1.567	11.0
-1	2.767*	2.467*	10.8 *	1.942	1.826	5.9
0	0.816†	0.378†	53.7 †	5.349	5.257	1.7
1	2.423	2.149	11.3	1.715	1.523	11.2
2	1.869	1.649	11.8	1.174	0.952	18.9
3	3.593	3.464	3.6			
4.0 Å						
-3	4.014	3.597	10.4	1.501	1.380	8.0
-2	2.305†	2.340†	-1.5†	1.790	1.628	9.1
-1	2.826*	2.556*	9.6*	1.958	1.860	5.0
0	0.833†	0.435†	47.7 †	5.362	5.282	1.5
1	2.442	2.192	10.2	1.755	1.607	8.4
2	1.883	1.678	10.9	1.222	1.054	13.8
3	3.598	3.476	3.4	1.920	1.825	5.0
4.2 Å						
-3	-5.723	3.535	161.8	1.506	1.392	7.6
-2	2.230†	2.283†	-2.4 †	1.799	1.645	8.5
-1	-2.514*	2.653*	205.5*	1.962	1.869	4.7
0	3.603‡	0.005‡	99.9‡	5.365	5.289	1.4
1	-2.170*	3.257*	250.1*	1.762	1.623	7.9
2	2.275†	1.203†	47.1†	1.231	1.072	12.9
3	-5.314	3.489	165.7	1.924	1.833	4.7
30 ˚						
-3	4.194	4.024	4.0	1.732	1.640	5.3
-2	2.232	2.225	0.3	1.742	1.637	6.0
-1	2.989	2.791	6.6	1.981	1.909	3.6
0	0.457†	0.264†	42.2 †	5.379	5.317	1.2
1	3.583*	3.475*	3.0*	1.804	1.710	5.2
2	1.434†	1.291†	10.0 †	1.277	1.167	8.6
3	3.618	3.518	2.7	1.920	1.825	5.0
60 ˚						
-3	4.300	4.248	1.2	1.793	1.763	1.6
-2	2.228	2.179	2.2	1.804	1.762	2.3

-1	3.060	3.004	1.8	2.016	1.979	1.8
0	1.192	1.142	4.2	5.402	5.363	0.7
1	2.501	2.440	2.5	1.860	1.822	2.0
2	2.089	2.040	2.4	1.350	1.314	2.7
3	3.645	3.575	1.9	1.974	1.934	2.0
90°						
-3	4.316	4.280	0.8	1.595	1.573	1.4
-2	2.198	2.151	2.1	1.922	1.897	1.3
-1	3.147	3.114	1.1	2.025	1.997	1.4
0	1.117	1.082	3.1	5.408	5.376	0.6
1	2.643	2.610	1.3	1.872	1.846	1.4
2	2.041	1.999	2.0	1.364	1.343	1.6
3	3.658	3.602	1.6	1.985	1.956	1.4

1,4-bis{4-{(E)-4-thiostyryl}}benzene) in vacuum, and in junction. Energies are given in eV. The differences between the vacuum and junction calculations are given in percent.
†: Either E_{n-1} or E_{n+1} is obtained from linear least squares fittings.
‡: Both E_{n-1} and E_{n+1} are obtained from linear least squares fittings.
⋆: E_n is obtained from linear least squares fitting

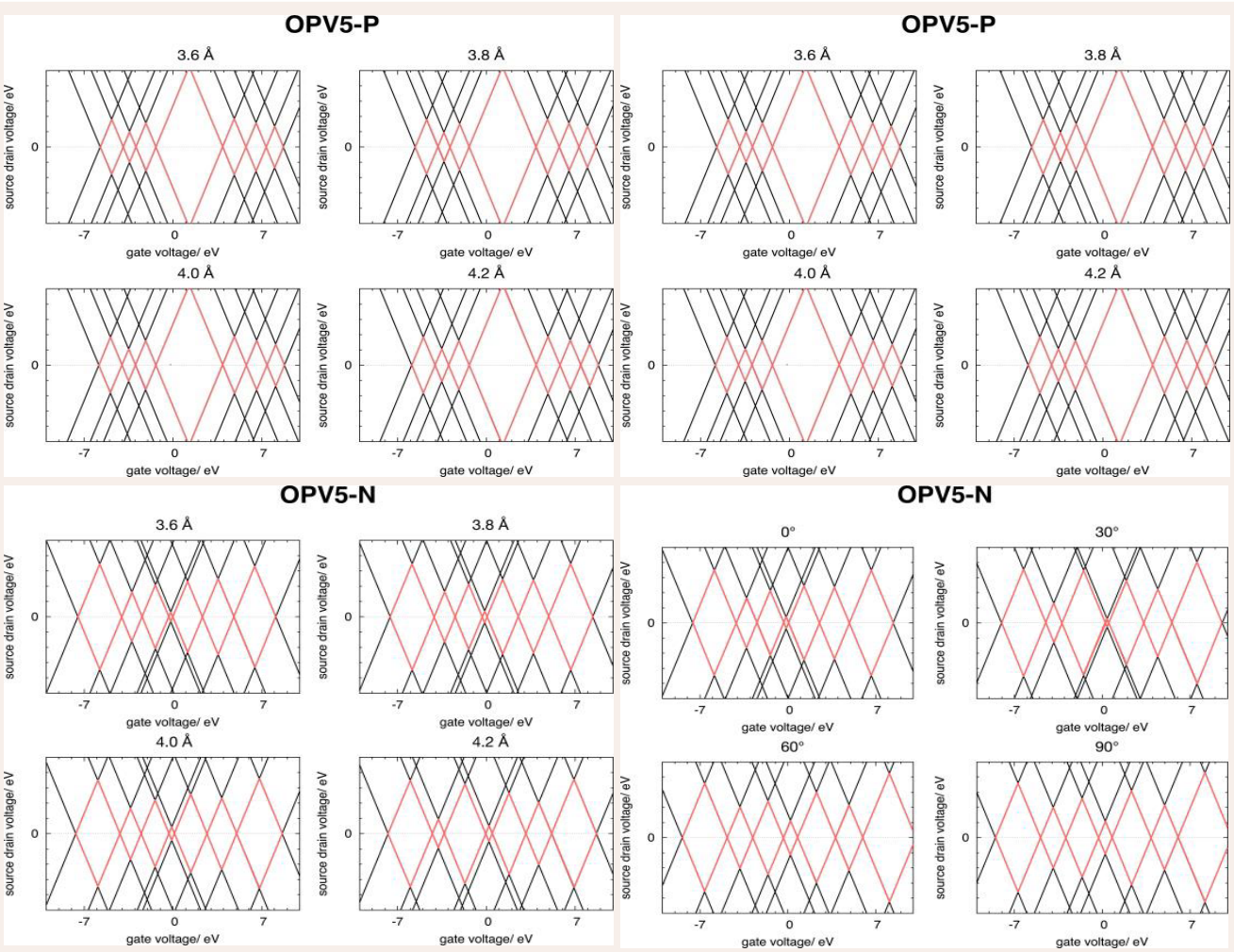

Figure 2 Coulomb blockade diamonds of OPV5-P((E,E)- 1,4-bis{4-{(E)-4-(tert-butylthio)styryl}}benzene) (top) and OPV5-N ((E,E)-1,4-bis{4-{(E)-4-thiostyryl}}benzene) (bottom) at different distances (left) and rotations (right) in the junction. The calculations are performed at static polarizability (Δα=0), hence, the diamonds are calculated according to Eq.(9). The Coulomb blockade diamonds for the redox states (molecular charge: q=-3,-2,-1,0,1,2,3 from left to right) are marked with red.

This is be due to the fact that covalent bonds can be formed from sulfur atom to the electrode when protecting groups are not present. Covalent bonds between the molecule and the electrode are not included in the calculations. However, it is encountered for through the strong polarization from gold on the negatively charged sulfur atoms at the ends of the molecule.

We compare the calculated Coulomb blockade diamonds with those achieved by experiment and we note strong similarities with the measured data for different redox states. There is a remarkable similarity of the three center diamonds (+1, 0, -1) of OPV5-P from calculations and in experiment. However, the remaining calculated diamonds of OPV5-P (+3, +2, -2, -3) show very little resemblance to experiment. On the other hand, the calculated diamonds of OPV5-N show increased similarity to experiment, where the calculated diamonds of OPV5-P deviate. These results indicate that the experiments performed at high gate volt- age may actually result in dissociation of the protecting groups on OPV5-P's, and form a structure similar to OPV5-N. Therefore we conclude that the high gate voltages break the covalent bonds of the protecting butyl groups of OPV5-P, resulting in a structure similar to OPV5-N.

CONCLUSION

The study is performed using a QM/MM method. Chemical features of both OPV5-P and OPV5-N, in junction, are investigated for different orientation of the molecular systems between the two gold nanoparticles. Coulomb blockade diamonds are explicitly constructed using a Poisson approach coupled to a QM/MM method. Results from these inexpensive calculations show electrochemistry on the single molecule level. In addition, remarkable resemblances to experimental data are observed. However, more surprising is the fact that the results indicate changes in chemical structure of the OPV5 molecule at high gate voltage.

REFERENCES

1. Kubatkin S, Danilov A, Hjort M, Cornil J, Bredas JL, Stuhr-Hansen N, et al. Single-electron transistor of a single organic molecule with access to several redox states. Nature. 2003; 425: 698-701.
2. Aviram A, Ratner MA. Molecular rectifiers. Chem Phys Let. 1974; 29: 277- 283.
3. Carroll RL, Gorman CB. The genesis of molecular electronics. Angew Chem Int Ed. 2002; 41: 4378-4400.
4. Katsonis N, Kudernac T, Walko M, van der Molen SJ, van Wees BJ, Feringa BL. Reversible Conductance Switching of Single Diarylethenes on a Gold Surface. Adv Mater. 2006; 18: 1397-1400.
5. van der Molen SJ, Liao J, Kudernac T, Agustsson JS, Bernard L, Calame M, et al. Electrochemical control of quantum interference in anthraquinone-based molecular switches. Nano Lett. 2008; 9: 76-80.
6. Kim Y, Hellmuth TJ, Sysoiev D, Pauly F, Pietsch T, Wolf J, et al. Current–voltage characteristics of single-molecule diarylethene junctions measured with adjustable gold electrodes in solution. Nano Lett. 2012; 12: 3736-3742.
7. James DK, Tour JM. Preparation of High Quality Electrical Insulator Self-Assembled Monolayers on Gold. Experimental Investigation of the Conduction Mechanism through Organic Thin Films. Chem Mater. 2004; 16: 4423-4435.
8. Nitzan A, Ratner MA. Electron transport in molecular wire junctions Science. 2003; 300: 1384-1389.
9. Heath J, Ratner M. Electronic transport in metal-molecular nanoelectronic networks: A density functional theory study. PHYSICS TODAY. 2003; 56: 43-49.
10. 10. . McCreery RL. Molecular Electronic Junctions. Chem Mater. 2004; 16: 4477-4496.
11. Bowler D. Atomic-scale nanowires: physical and electronic structure. J Phys Nanoscale Condens Matter. 2004; 16: R721.
12. Nitzan A. RVB Contribution to Superconductivity in MgB2arXiv preprint. Cond-mat. 2001.
13. Beaujuge PM, Frechet MJ. Molecular Design and Ordering Effects in π-Functional Materials for Transistor and Solar Cell Applications. J Amer Chem Soc. 2011; 133: 20009-20029.
14. Sanchez C, Belleville P, Popall M, Nicole L. Applications of advanced hybrid organic–inorganic nanomaterials: from laboratory to market. Chem Soc Rew. 2011; 40: 696-753.
15. Zrimsek AB, Chiang N, Mattei M, Zaleski S, McAnally MO, Chapman CT, et al. Single-Molecule Chemistry with Surface- and Tip-Enhanced Raman Spectroscopy. Chem Rev. 2017; 117: 7583-7613.
16. Casalini S, Bortolotti CA, Leonardi F, Biscarini F. Multiscale Sensing of Antibody–Antigen Interactions by Organic Transistors and Single-Molecule Force Spectroscopy. Chem Soc Rev. 2017; 46: 40-71.
17. Liu X, Sangtarash S, Reber D, Zhang D, Sadeghi H, Shi J, et al. Gating of Quantum Interference in Molecular Junctions by Heteroatom Substitution. ANGE- WANDTE Chemie Int Ed. 2017; 56: 173-176.
18. Oh JY, Rondeau-Gagne S, Chiu YC, Chortos A, Lissel F, Wang GJN, et al. Intrinsically stretchable and healable semiconducting polymer for organic transistors. Nat. 2016; 39: 411-415.
19. Guo C, Wang K, Zerah-Harush E, Hamill J, Wang B, Dubi Y, Xu B. Sub-nanometer supramolecular rectifier based on the symmetric building block with destructive σ-interference. Nat Chem. 2016; 8: 484-490.
20. Xiang D, Wang X, Jia C, Lee T, Guo X. Molecular-Scale Electronics: From Concept to Function. Chem Rev. 2016; 116: 4318-4440.
21. Michaelson HB. The work function of the elements and its periodicity. J Appl Phys. 1977; 48: 4729-4733.
22. Olsen ST, Arcisauskaite V, Hansen T, Kongsted J, Mikkelsen KV. Computational assignment of redox states to Coulomb blockade diamonds. Phys Chem Chem Phys. 2014; 16: 17473-17478.
23. Olsen ST, Hansen T, Mikkelsen KV. First hyperpolarizability of para-aminoaniline induced by a variety of gold nano particles. Theor Chem Acc. 2011; 130: 839-850.
24. Olsen ST, Hansen T, Kongsted J, Mikkelsen KV. Linear response functions for coupled cluster/molecular mechanics including polarization interactions. Chemical Physics. 2015; 459: 40-44.
25. Danilov A, Kubatkin S, Kafanov S, Hedegård P, Stuhr- Hansen N, Moth-Poulsen K, et al. Orientation-Dependent Performance Analysis of Benzene/Graphene-Based Single-Electron Transistors Nano letters. 2008; 8: 1-5.
26. Arcisauskaite V, Kongsted J, Hansen T, Mikkelsen KV. Role of metal-nanostructure features on tip-enhanced photoluminescence of single molecules. Chemical Physics Letters. 2009; 470: 285-288.
27. Aidas K, Angeli C, Bak KL, Bakken V, Bast R, Boman L, et al. The Dalton quantum chemistry program system.Wiley Interdiscip Rev Comput Mol Sci. 2014; 4: 269-284.
28. Yanai T, Tew DP, Handy NC. Matrix Isolation and Computational Study

on the Photolysis of CHCl2COCl. Chem Phys Lett. 2004; 393: 51-57.

29. Dunning TH Jr. Gaussian basis sets for use in correlated molecular calculations. I. The atoms boron through neon and hydrogen J Chem Phys. 1989; 90: 1007-1023.

30. Hansen T, Hansen V, Arcisauskaite, Mikkelsen KV, Kongsted J, Mujica V. THEORETICAL QUANTIFICATION OF THE MODIFIED PHOTOACTIVITY OF J Phys Chem C. 2010; 114: 20870–20876.

31. Olsen ST, Hansen T, Mikkelsen KV. Unconventional photon blockade from bimodal driving and dissipations in coupled semiconductor microcavities J Chem Physics. 2017; 146: 104306.

32. Cobden DH, Nygård J. Shell Filling in Closed Single-Wall Carbon Nanotube Quantum Dots Physical Rev Lett. 2002.

Cite this article

Prestholm I, Olsen ST, Hansen T, Mikkelsen KV (2022) Theoretical Investigation of OPV5's Transport Properties in the Coulomb Blockade Regime. Chem Eng Process Tech 7(1): 1064.